

**Electronic Supplementary Information**

Elucidating proline dynamics in spider dragline silk fibre using  $^2\text{H}$ - $^{13}\text{C}$  HETCOR MAS NMR

Xiangyan Shi, Jeffery L. Yarger\* and Gregory P. Holland\*

*Department of Chemistry and Biochemistry, Magnetic Resonance Research Center, Arizona State University,*

*Tempe, Arizona 85287-1604*

## Table of Contents:

### Materials and Methods

Fig. S1 Liquid-state  $^2\text{H}$  NMR spectrum of hydrolyzed U- $[\text{}^2\text{H}_7, \text{}^{13}\text{C}_5, \text{}^{15}\text{N}]$ -Pro labeled *A. aurantia* dragline spider silk

Fig. S2 Simulated  $^2\text{H}$  quadrupole line shapes for deuterium undergoing fast reorientation between two sites separated by an angle  $\theta$

Fig. S3  $^{13}\text{C}$ -detected Pro  $^2\text{H}$   $T_1$  inversion recovery curves for U- $[\text{}^2\text{H}_7, \text{}^{13}\text{C}_5, \text{}^{15}\text{N}]$ -Pro labeled *A. aurantia* dragline silk

Calculating molecular motional rate using  $^2\text{H}$   $T_1$

Fig. S4  $^2\text{H}$  one-pulse MAS NMR spectrum (black) and its fit (green) for wet, supercontracted U- $[\text{}^2\text{H}_7, \text{}^{13}\text{C}_5, \text{}^{15}\text{N}]$ -Pro labeled *A. aurantia* dragline silk

### References

## Materials and Methods

### *Sample Preparation*

*A. aurantia* dragline silk was collected from adult female spiders using the forcible silking method as described in previous studies.<sup>S1</sup> The silking process was monitored under a microscope to avoid contamination from minor ampullate silk. The U-[<sup>2</sup>H<sub>7</sub>,<sup>13</sup>C<sub>5</sub>,<sup>15</sup>N]-Pro labeled dragline silk were obtained from *A. aurantia* spiders fed with 30-40  $\mu$ l 16% (w/v) U-[<sup>2</sup>H<sub>7</sub>,<sup>13</sup>C<sub>5</sub>,<sup>15</sup>N]-Pro (Cambridge Isotopes, Andover, MA) during every silking process. The spiders were fed with crickets once a week. The dry silk sample refers to material used without any further processing after collecting from spiders. Supercontracted (wet) silk samples were soaked in deuterium-depleted water for at least 2 hours to achieve saturation prior to NMR experiments.

### *NMR Spectroscopy*

Solid-state NMR experiments were conducted on a Varian VNMRS 400 MHz spectrometer equipped with a 3.2 mm MAS probe operating in triple resonance mode (<sup>1</sup>H/<sup>13</sup>C/<sup>2</sup>H) at room temperature (25 °C). Sample heating due to MAS results in an actual sample temperature of 30 °C (temperature was calibrated with lead nitrate<sup>S2</sup>). <sup>2</sup>H-<sup>13</sup>C MAS HETCOR and <sup>2</sup>H T<sub>1</sub> indirect detection experiments were set up as described in a recent publication.<sup>S3</sup> In the <sup>2</sup>H-<sup>13</sup>C HETCOR experiments, 91 kHz (2.75  $\mu$ s  $\pi/2$  pulse) <sup>2</sup>H rf field was employed and a  $\sim$ 2 kHz <sup>2</sup>H GARP decoupling was utilized during signal acquisition. The <sup>13</sup>C and <sup>2</sup>H chemical shifts were indirectly referenced to the adamantane downfield resonance at 38.56 ppm and the D<sub>2</sub>O resonance at 4.788 ppm, respectively. Experiments were performed using 10 kHz MAS spinning rate and the following additional parameters:

- 2D <sup>2</sup>H-<sup>13</sup>C HETCOR CP-MAS experiment: 25 kHz sweep width in <sup>13</sup>C dimension, 500 kHz sweep width with 256 t<sub>1</sub> points in <sup>2</sup>H dimension, 40.96 ms acquisition time, 2 ms <sup>2</sup>H-<sup>13</sup>C CP contact time, a recycle delay of 2.5 s and 224 scans. In order to obtain <sup>2</sup>H-<sup>13</sup>C chemical shift correlation spectrum with higher resolution, another 2D <sup>2</sup>H-<sup>13</sup>C HETCOR CP-MAS experiment with rotor-synchronized sampling in <sup>2</sup>H dimension was performed using 10 kHz sweep width with 64 t<sub>1</sub> points in <sup>2</sup>H dimension.

-  $^{13}\text{C}$ -detected  $^2\text{H}$   $T_1$  measurement through  $^2\text{H}$ - $^{13}\text{C}$  HETCOR CP-MAS: A composite  $\pi$  pulse  $((\pi/4)_x-(\pi)_y-(\pi/2)_x-(\pi)_y-(\pi/4)_x)$  is used as the  $^2\text{H}$  inversion pulse in the pulse sequence.<sup>S3</sup> The additional experimental parameters were 25 kHz sweep width, 40.96 ms acquisition time, 2 ms  $^2\text{H}$ - $^{13}\text{C}$  CP contact time, 5 s recycle delay time and 512 scans.

-  $^2\text{H}$  solid-echo MAS experiment: 500 kHz sweep width, 40.96 ms acquisition time, a recycle delay of 3 s and 2944 scans. The rotor-synchronized delay between the two  $\pi/2$  pulses was 100  $\mu\text{s}$  (rotor-synchronized for 10 kHz MAS). 20  $\mu\text{s}$  delay was set between the second  $\pi/2$  pulse and the beginning of acquisition. The acquired FID was left shifted 46 points to the echo maximum prior to Fourier transform in order to correct spectrum phase.

-  $^2\text{H}$  one-pulse MAS experiment: 500 kHz sweep width, 40.96 ms acquisition time, a recycle delay of 4 s and 2944 scans. 20  $\mu\text{s}$  delay was set between the  $\pi/2$  rf pulse and the beginning of acquisition. During data process, the raw FID was left shifted 49 points to eliminate spectrum phase distortion caused by probe ringdown.

1D  $^2\text{H}$  liquid-state NMR data was collected on an Agilent Inova 500 MHz spectrometer equipped with a 5 mm Inverse Detect Broadband PFG Probe. The experiment was performed on U- $[^2\text{H}_7, ^{13}\text{C}_5, ^{15}\text{N}]$ - Pro labeled silk. About 1 mg silk sample was hydrolyzed in 6 M HCl for 2 days under 108 °C, then reconstituted in 700  $\mu\text{l}$   $\text{H}_2\text{O}$  and transferred to 5 mm NMR tube. Data was acquired using the lock channel. The NMR pulse sequence is a  $\pi/2$  deuterium excitation pulse followed by data acquisition. Additional experiment parameters are: 1535.63 Hz sweep width, 2.049 ms acquisition time and a recycle delay of 5s.

### *$^2\text{H}$ NMR line shape simulation*

Deuterium MAS quadrupole line shapes were simulated using SPINEVOLUTION 3.4.4 software packages.<sup>S4</sup> All simulations were conducted with the ASG powder orientation calculation scheme. For proline in dry silk, the MAS line shapes were calculated using a  $\text{CD}_2$  group undergoing fast two-site reorientations with  $C_Q=170$  kHz and  $\eta=0$ .<sup>S5</sup> Simulations were performed for various two-site reorientation angles to find the best one matching with experimental data for the different  $\text{CD}_2$  groups on the proline sidechain. A deuterium three-

site reorientation model was used to simulate the microsecond proline backbone motion occurring in supercontracted (wet) silk. The averaged EFG principle axis system was set to reorient between  $(\theta, 0)$ ,  $(\theta, 120)$  and  $(\theta, 240)$ . Simulations were performed with various  $\theta$  and reorientation rates and compared with experimental data to find the best match.

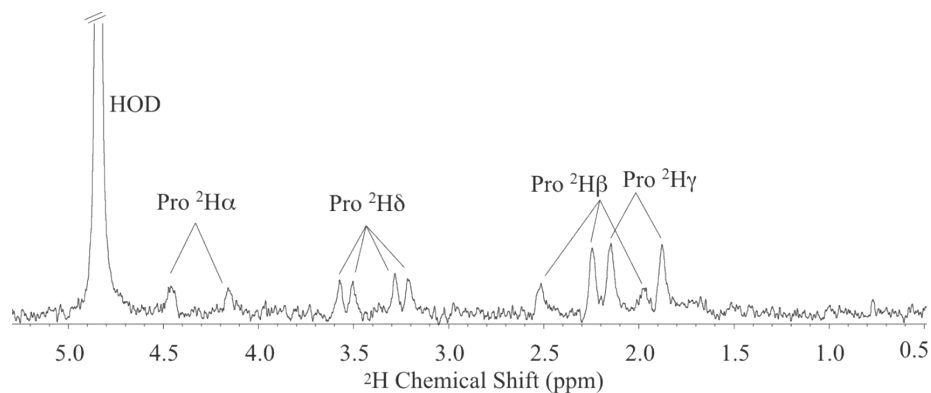


**Fig. S1** Liquid-state  $^2\text{H}$  spectrum of hydrolyzed U- $[^2\text{H}_7, ^{13}\text{C}_5, ^{15}\text{N}]$ -Pro labeled *A. aurantia* dragline silk. Silk collected from spiders fed with U- $[^2\text{H}_7, ^{13}\text{C}_5, ^{15}\text{N}]$ -Pro aqueous solution. One-bond  $^2\text{H}$ - $^{13}\text{C}$   $J$ -splitting peak patterns are observed for Pro  $\alpha$ ,  $\beta$ ,  $\gamma$  and  $\delta$  groups. The corresponding  $J_{^2\text{H}-^{13}\text{C}}$  constant is 23.4 Hz, 20.9 Hz, 20.6 Hz and 22.6 Hz for  $\alpha$ ,  $\beta$ ,  $\gamma$  and  $\delta$  group, respectively. The  $J$ -splitting effect (5.5 Hz) caused by  $^{15}\text{N}$  is also observed for  $^2\text{H}\delta$ . These  $J$ -splitting peak patterns indicate that Pro is selectively labeled by  $^2\text{H}$ - $^{13}\text{C}$  pairs at the different sites and no additional deuterium labeling occurred for any other amino acid to any appreciable extent.

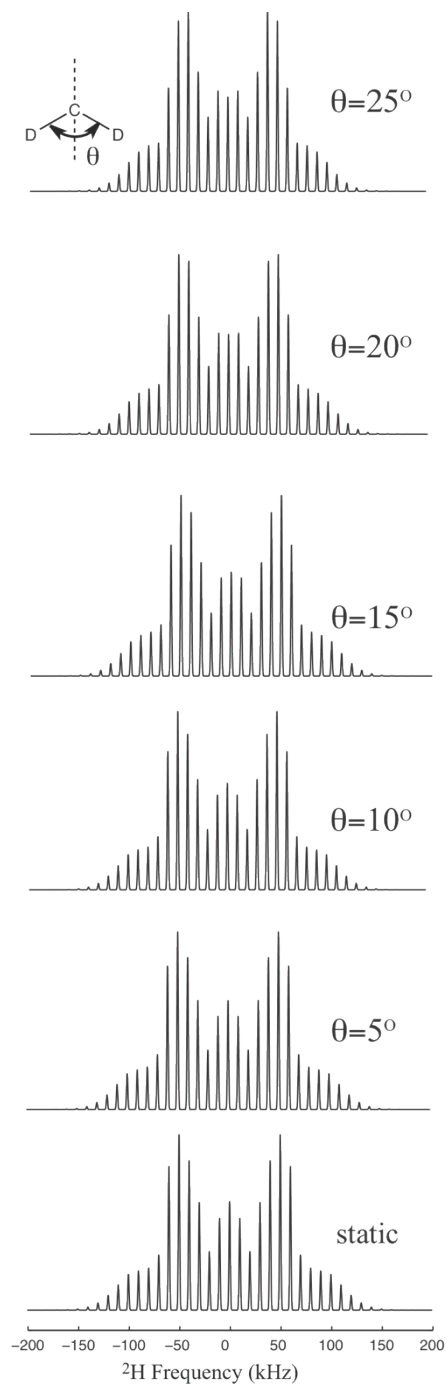


**Fig. S2** Simulated  $^2\text{H}$  quadrupole line shapes for deuterium undergoing fast reorientation between two sites separated by  $\theta$ . Simulations were conducted using SPINEVOLUTION software<sup>S4</sup> with  $C_Q=170$  kHz and  $\eta=0$ <sup>S5</sup>. In the current paper, Pro  $^2\text{H}$  molecular motions were proposed by comparing experimental deuterium line shapes with these simulations.

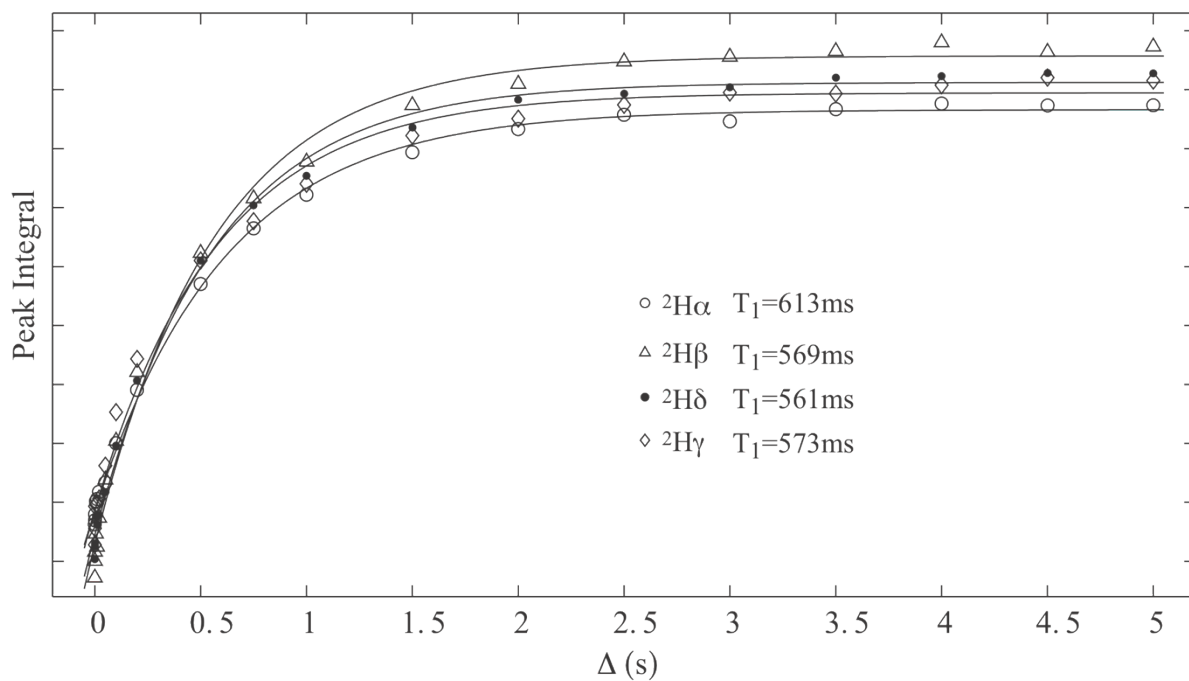


**Fig. S3**  $^{13}\text{C}$ -detected Pro  $^2\text{H}$   $T_1$  inversion recovery curves for U- $[^2\text{H}_7, ^{13}\text{C}_5, ^{15}\text{N}]$ -Pro labeled *A. aurantia* dragline silk. The  $T_1$  for each deuterium of Pro is shown in the figure.



## Calculating molecular motional rate using $^2\text{H } T_1$

The quadrupolar interaction is the dominant spin relaxation mechanism for deuterium in solids. When the interaction is reduced by molecular motion of the considered group, a specific mathematical relation can be developed between deuterium  $T_1$  and the molecular motional rate. In present study,  $^2\text{H } T_1$ s were used to calculate molecular motional rate for Pro deuterium that undergo reorientation between two sites separated by an angle ( $\Theta$ ). The calculation process is as follows.

For Pro deuterium which undergoes two sites reorientation,<sup>S6</sup>

$$1/T_1 = (\omega_Q^2/8)A_1 \{ \tau/(1 + \omega^2 \tau^2)[B_4 - (0.75B_1 - B_2)\cos 2\varphi] + \tau/(1 + 4\omega^2 \tau^2)(4B_5 - 4B_2 \cos 2\varphi) \}$$

where,

$$A_1 = \sin^2(2\Theta)$$

$$B_1 = \sin^2(2\theta)$$

$$B_2 = \sin^4(\theta)$$

$$B_4 = \cos^2(\theta) + \cos^2(2\theta)$$

$$B_5 = \sin^2(\theta) + 0.25 \sin^2(2\theta)$$

$\Theta=12.5^\circ$ ,  $17.5^\circ$  and  $7.5^\circ$  for Pro  $^2\text{H}\beta$ ,  $^2\text{H}\gamma$  and  $^2\text{H}\delta$ , respectively, according to the  $^2\text{H}$  line shapes determined in the current work.  $\tau=(2k)^{-1}$  and  $k$  is the two sites reorientation rate. Pro  $^2\text{H}$  quadrupolar patterns are independent of  $\varphi$  because the quadrupolar asymmetry parameter  $\eta=0$ <sup>S5</sup> ( $(\theta, \varphi)$  are the polar angles that define the orientation of the external field in the crystal-fixed coordinate system). Thus, for a specific  $\theta$ , one would find,

$$1/T_1 = \frac{\int_0^{2\pi} (\omega_Q^2/8)A_1 \{ \tau/(1 + \omega^2 \tau^2)[B_4 - (0.75B_1 - B_2)\cos 2\varphi] + \tau/(1 + 4\omega^2 \tau^2)(4B_5 - 4B_2 \cos 2\varphi) \} d\varphi}{\int_0^{2\pi} 2\pi d\varphi}$$

$$= (\omega_Q^2/8)A_1 [ \tau/(1 + \omega^2 \tau^2)B_4 + \tau/(1 + 4\omega^2 \tau^2)4B_5 ]$$

Using the experimentally measured  $T_1$ , the two sites reorientation rate can be calculated using the above equation for the case of a specific  $\theta$ . In the current work, for each deuterium on Pro side chain, the two sites reorientation rate is considered as the average of the rates of two cases -  $\theta=0$  and  $\theta=2\pi$ .

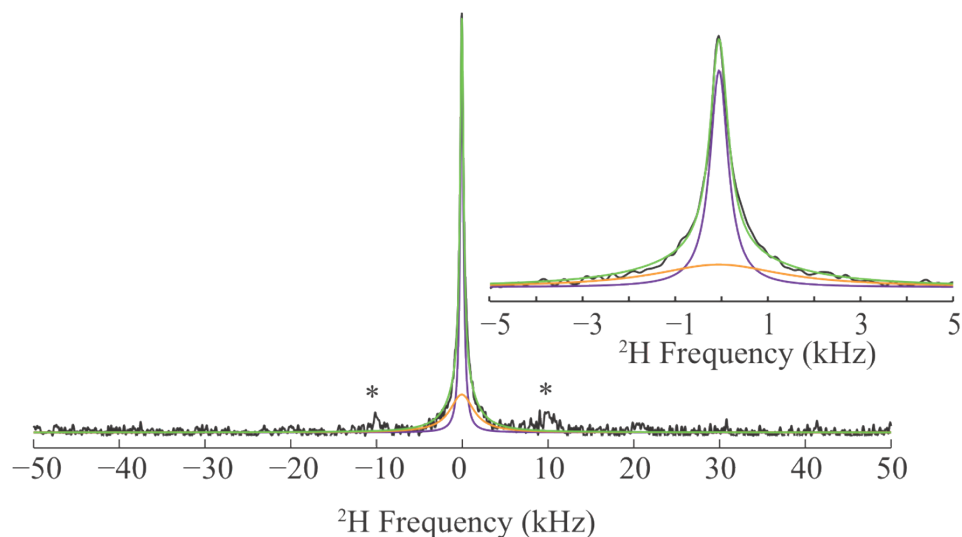


**Fig. S4**  $^2\text{H}$  one-pulse spectrum (black) and its fit (green) for wet, supercontracted U- $[^2\text{H}_7, ^{13}\text{C}_5, ^{15}\text{N}]$ -Pro labeled *A. aurantia* dragline silk. Two components were extracted from the fit – a broad peak (orange) and a narrow peak (purple). The asterisks mark the weak spinning sidebands. The fitting process is the same as that shown in Fig. 3 in the current article and the result is similar because the number of left shifts required to eliminate probe ring down were on the same time scale as the solid-echo delays (see Materials and Methods, above). The central peak is extremely broadened where the signal intensity is smaller than half maximum. The peak can not be fit with a single peak having Lorentzian, Gaussian or a combined line shape. This implies the existence of the broad component. The peak can be fit well to a combination of a broad (FWHM = 3.8 kHz) and narrow component (FWHM = 400 Hz) similar to the solid-echo data in the paper, Fig. 3. The fittings were performed using DMFit software to extract the narrow and broad component.<sup>S7</sup>

## References

- S1 R. W. Work and C. T. Young, *J. Arachnol.*, 1987, **15**, 65-80.
- S2 A. Bielecki and D. P. Burum, *J. Magn. Reson.*, 1995, **116**, 215-220.
- S3 X. Shi, J. L. Yarger and G. P. Holland, *J. Magn. Reson.*, 2013, **226**, 1-12.
- S4 M. Veshtort and R. G. Griffin, *J. Magn. Reson.*, 2006, **178**, 248-282.
- S5 S. K. Sarkar, P. E. Young and D. A. Torchia, *J. Am. Chem. Soc.*, 1986, **108**, 6459-6464.
- S6 D. A. Torchia, *J. Magn. Reson.*, 1982, **49**, 107-121.
- S7 D. Massiot, F. Fayon, M. Capron, I. King, S. Le Calvé, B. Alonso, J. O. Durand, B. Bujoli, Z. Gan, G. Hoatson, *Magn. Reson. Chem.* **2002**, *40*, 70-76.